Effect of Vibrations on the C 1s Photoemission in Formaldehyde in the Shape Resonance Region

Effect of vibrations on C 1*s* photoemission in formaldehyde in the shape resonance region

A. De Fanis,[1] D. A. Mistrov,[2] M. Kitajima,[3] M. Hoshino,[3] H. Shindo,[3] T. Tanaka,[3] H. Tanaka,[3] Y. Tamenori,[1]
A. A. Pavlychev,[2,4] and K. Ueda[4,*]

[1]*Japan Synchrotron Radiation Research Institute, Sayo-gun, Hyogo 679-5198, Japan*
[2]*Institute of Physics, St. Petersburg State University, 198504 St. Petersburg, Russia*
[3]*Department of Physics, Sophia University, Tokyo 102-8544, Japan*
[4]*Institute of Multidisciplinary Research for Advanced Materials, Tohoku University, Sendai 980-8577, Japan*

The vibrationally resolved C 1*s* single-hole ionization cross sections of H_2CO are measured in the region of the σ^* shape resonance. The energy of the shape resonance is pushed down by the excitation of the C-O stretching vibration v_2'. Our calculations, which take account of elastic multiple scattering within the C-O potential box, show that the downward shift of the shape resonance energy is originated from the elongation of the characteristic internuclear C-O distance in the core-ionized molecule with an increase in v_2'. The characteristic internuclear distance varies from $R^+(0,0,0) = 1.198$ Å up to $R^+(0,2,0) = 1.415$ Å. In addition to the elastic multiple-scattering mechanism, the internal inelastic scattering of the C 1*s* photoelectron by valence electrons is suggested as a possible mechanism responsible for the enhancement of vibrational excitations through the shape resonance and near threshold.

PACS number(s): 33.20.Rm, 33.20.Tp, 33.60.Fy

I. INTRODUCTION

Shape resonances are the most intriguing processes in molecular photoionization [1,2]. They are generally described in terms of trapping of the ejected photoelectrons by potential barriers of the molecular ion, with subsequent tunneling into the continuum. Recent progress in *K*-shell photoemission highlights the effects of molecular vibrations on shape resonances because their dependence on the final vibrational state (v') of the absorber is revealed. A typical example of these effects can be seen in the carbon monoxide [3–6]. The σ^* shape resonances observed in x-ray absorption spectra of CO above both the C and O 1*s* thresholds are also present in the C and O 1*s* single-hole-ionization (SHI) cross sections for the individual vibrational components v'. Through various observations [3–5], it is now well known that the energy of the σ^* shape resonance depends on v'. Mistrov *et al.* [4] exhibited, both experimentally and theoretically, that the energy of the v'-resolved shape resonance moves close to the C 1*s* threshold, and away from the O 1*s* threshold, with an increase in v', and interpreted this site-selective v' dependence of the resonance energy as the variation of characteristic internuclear distances for different vibrational components of C 1*s* and O 1*s* ionized states, with the help of a harmonic potential approximation for the relevant states, taking into account the interference of multiply scattered photoelectron waves.

In the present work, we discuss the relationship between molecular vibrations and the shape resonance in polyatomic systems. For such a purpose, we focus on the vibrational excitations that accompany C 1*s* photoionization in the formaldehyde molecule H_2CO. The ground-state electronic configuration of H_2CO is

$$1a_1(\text{O } 1s)^2 2a_1(\text{C } 1s)^2 3a_1^2 4a_1^2 1b_2^2 1b_1^2 2b_2^2 2b_1(\pi^*)^0$$

$$5a_1(\sigma^*)^0 (X\,{}^1A_1).$$

Ultraviolet and x-ray photoelectron spectroscopy (UPS and XPS) studies of H_2CO were reported some time ago [7–10]. C 1*s* electron energy loss and photoabsorption spectra were observed by Hitchcock and Brion [11] and by Remmers *et al.* [12], respectively, whereas C 1*s* SHI and C 1*s* total ionization cross sections were measured by Kilcoyne *et al.* [13]. Above the C 1*s* threshold, the dipole-allowed transition from the $2a_1(\text{C } 1s)$ orbital to the a_1 continuum orbital exhibits the $2a_1 \rightarrow 5a_1$ σ^* shape resonance. This resonance is interpreted as a result of elastic multiple scattering of the C 1*s* photoelectron on the oxygen and carbon atoms within the molecule. The amplitudes of backscattered waves on the hydrogen atoms are weak and their influence on the intramolecular interference is usually negligible [14]. Then the C 1*s* photoelectron wave function of H_2CO depends exclusively on the internuclear C-O separation. Within this assumption (referred to as the elastic multiple-scattering model hereafter), the difference in the shape resonance energies for H_2CO and CO is attributed to the difference in the C-O bond length. This idea was in fact the background of the bond-length-with-a-ruler method [15]. To what extent the bond-length-with-a-ruler method works is still a subject of debate, with both evidence favoring this method and indications that its application to extract bond lengths from excess energy positions of the shape resonance is at best unsafe (see, e.g., [1]). To investigate the effect of the shape resonance on specific vibrational components of the core-ionized states can be very instructive from the point of view of the debate regarding the bond-length-with-a-ruler method because different vibrational components probe different characteristic C-O distances for H_2CO, as discussed in detail by Mistrov *et al.* [4] for CO. These investigations have shown that the energy of the shape

---

*Electronic address: ueda@tagen.tohoku.ac.jp

resonance cannot be unambiguously linked to a single C-O equilibrium distance in the ground state. In addition to many-electron effects, this energy is noticeably influenced by the vibrational excitations accompanying inner-shell ionization. Thus, information obtained in the present work on H_2CO provides deeper understanding of the relationships between the position of the shape resonance and interatomic separation. In addition to the C-O stretching vibrations, in the case of H_2CO the CH_2 scissor and the C-H stretching vibrations can also be involved in molecular dynamics and may affect the C 1s photoemission dynamics.

In order to examine the above-described multiple-scattering model and understand furthermore to what extent the complexity of molecular dynamics influences the C 1s photoemission in H_2CO, in comparison with CO [4], we have carried out vibrationally resolved measurements of C 1s photoemission in the shape resonance region. The influence of the C-O stretching vibrations on the shape resonance energy observed here is well reproduced by the present calculations. Possible mechanisms responsible for the enhancement of other modes will be qualitatively discussed.

II. EXPERIMENT

A. Experimental procedure

The experiments were conducted at the c branch of the soft x-ray photochemistry beamline 27SU [16] at SPring-8, the 8 GeV synchrotron radiation facility in Japan. The monochromator installed in this beamline is of Hettrick type and a resolution of between 10 000 and 20 000 can be achieved [17]. The light source is a figure-8 undulator [18], with which one can perform angle-resolved electron spectroscopy by switching the direction of polarization from horizontal to vertical, and vice versa, only by adjusting the gap of the undulator. The degree of light polarization was confirmed to be greater than 0.98 for both directions by measurement of the 2s and 2p photoelectrons of Ne for the present optical setting [19]. The monochromator slits were set to values corresponding to a photon energy width of about 50 meV. The electron spectrometer employed is manufactured by GammaData-Scienta (SES-2002). It consists of a hemispherical electron analyzer with a Herzog-plate termination and accelerating-retarding multielement lens, as well as with a gas cell (GC-50), which are installed in the differentially pumped chamber [20]. For these particular measurements, the analyzer was operated at a pass energy of 10 eV, and with a slit setting of 1.5 mm, which correspond to approximately 50 meV electron energy width. Each individual spectrum was recorded for approximately 10 min; this time is sufficiently short that a possible slow photon energy drift causes negligible additional broadening to the observed structure.

In the present measurements, the C 1s and photoelectron spectra of H_2CO were recorded at excess energies of between 17.87 and 2.78 eV. Formaldehyde in its dimerized form, i.e., *para*-formaldehyde, was purchased from Wako, Japan, with a stated purity of 97%, and was degassed by repeated freezing under a pressure of 10^{-4} Pa without further purification. The formaldehyde target beam was prepared directly from the *para*-formaldehyde by heating a bottle con-
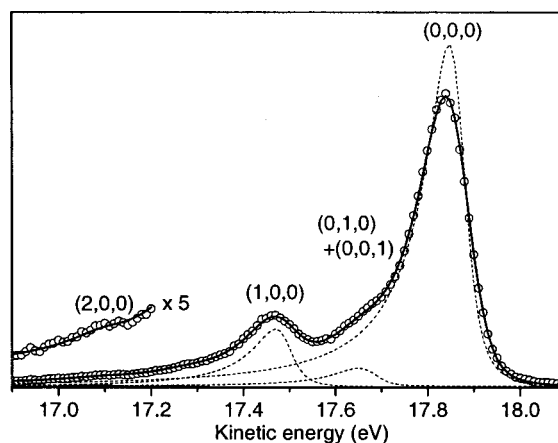

FIG. 1. C 1s photoelectron spectrum of H_2CO at the photon energy of 312.22 eV. Dots, measured spectrum; solid line, least-χ^2 fit; dashed lines, individual components of the fitting but without the instrumental broadening.

taining the solid sample to 50–65 °C. At this temperature, a background pressure of 10^{-4} Pa (uncorrected for the ionization efficiency of formaldehyde) was measured in the experimental chamber, in which the gas cell is placed. A plug of glass wool was placed over the powder in the reservoir to prevent the powder from dispersing during warming or pumping of the reservoir. All tubing from the reservoir to the gas cell was heated to 60 °C to prevent condensation and possible polymerization of the formaldehyde vapor in the inlet lines. The whole electron spectrometer apparatus was kept at 65 °C during the measurement. Assuming equilibrium conditions apply, the dimer-monomer ratio was estimated to be 10^{-4} under the experimental conditions (10^{-4} Pa H_2CO pressure and 50 °C) and thus the contribution from dimers could be neglected.

B. Experimental results

The C 1s photoelectron spectrum of H_2CO measured at the photon energy of $h\nu=312.22$ eV, 17.87 eV above the C 1s ionization threshold, is presented in Fig. 1. The figure includes the spectrum at the magic angle, reconstructed from the measured angle-resolved spectra, and the corresponding least-χ^2 fit with the individual vibrational components. The spectrum at the magic angle $I(54.7°)$ is obtained from the angle-resolved spectra at 0° and 90° as $I(54.7°)=I(0°)+2I(90°)$. In addition to the intense main peak, at least three vibrationally excited bands are resolved. In H_2CO there are three a_1 totally symmetric vibrational modes: C-H stretching (v_1), C-O stretching (v_2), and CH_2 scissor (v_3). The vibrational frequencies of these modes in neutral H_2CO in the ground state are $\omega_1=345.0$, $\omega_2=216.5$, and $\omega_3=186.0$ meV [21]. We attribute the most intense component in the spectrum in Fig. 1 to (0,0,0), the component that peaks near 17.47 eV to (1,0,0), the one at 17.65 eV to the unresolved components $(0,1,0)+(0,0,1)$, and the small bump near 17.10 eV to (2,0,0).

Each angle-resolved spectrum was normalized by gas pressure and photon flux. The photon flux was measured by

a photocurrent on the refocusing mirror upstream of the gas cell. In the photon energy region of interest, the measurements of photon flux by the photocurrent suffer from carbon contamination on the surface of the optical components. This was corrected by comparing intensities of angle-resolved Ar $2p$ photoelectron spectra with their cross sections and angular distribution in the photon energy of interest. The transmission of the electron analyzer is not constant in this low-electron-energy region, and it was corrected by comparing Ar $2p$ photoelectron spectra with their cross sections and angular distribution in the kinetic energy region of interest. After these corrections, each angle-resolved electron spectrum was fitted. Each partial cross section was determined from the intensities of each individual component in the angle-resolved spectra. The effect of postcollision interaction was included by simulating the individual profiles with the equation of van der Straten *et al.* [22], convoluted with a Gaussian distribution to take into account the experimental broadening. The full width at half maximum of the Gaussian profile was fitted to about 70 meV.

From the result of the fit of the spectra at all energies the natural lifetime width Γ is 83(7) meV, independent of whether the fit is run in least-χ^2 or least-squares mode. Γ for the C 1s ionized state of H_2CO determined here can be compared with Γ for C 1s ionized states of other simple molecules (all in meV): 78(10) [23] and 95(5) [24] for CO; 78(15) [25] and 99(2) [26] for CO_2; 83(10) [27], 95(2) [28], and 97.4(2.0) [29] for CH_4; 77 for CF_4 [24]; 95 [30] and 85(10) [31] for C_2H_4; 106(2) for C_2H_2 [32]; 98(10) [33] and 100(2) for both C_2H_6 and C_2D_6 [34]; 89 for both CH_2F_2 and CHF_2Cl [35]. We intend to use the lifetime widths as the Γ parameters entering in the equation for the PCI profile [Eq. (8) of [22]]. In the limit of high excess energy, where the PCI becomes negligible, the line profile becomes asymptotically Lorentzian and Γ becomes the full width at half maximum of the Lorentzian distribution. The fitting procedure included all the components with $v_1 \leqslant 2$ and $v_2 + v_3 \leqslant 1$. No anharmonicity is considered. The intensities of the mixed components (1,1,0) and (1,0,1), as well as (2,1,0) and (2,0,1), were constrained to the product of the intensities for excitations of the independent vibrational progression. The vibrational frequency of the CH_2 symmetric stretching mode was treated as a free fitting parameter, determined to be 377(5) meV. The other two vibrational frequencies are too close to each other to extract them and their corresponding intensities, so they were fixed to their corresponding values in the neutral ground state. For this reason we cannot extract the individual intensities of the (0,1,0) and (0,0,1) vibrations but only their sum. The thin line that peaks near 17.65 eV in Fig. 1 is the sum of the PCI profiles for the (0,1,0) and (0,0,1) components.

Spectral dependences of the measured C 1s SHI cross sections σ^+, σ^+_{000}, σ^+_{100}, and $\sigma^+_{001+010}$ are presented in Fig. 2. Here the SHI cross section σ^+_{ijk} corresponds to the transition $(0,0,0) \rightarrow (i,j,k)$ accompanying the C 1s ionization. The total cross section σ^+ corresponds to the sum of the (0,0,0), (0,1,0), (0,0,1), (1,0,0), (1,1,0), (1,0,1), (2,0,0), (2,1,0), and (2,0,1) partial cross sections:

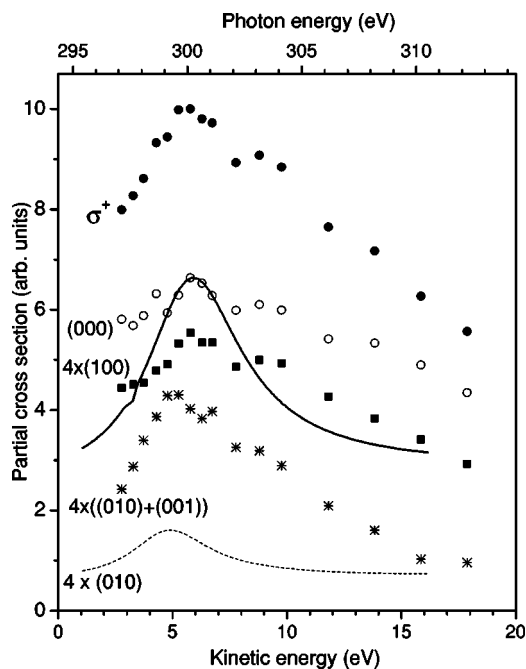FIG. 2. Measured C 1s SHI cross sections in H_2CO: σ^+_{000}, σ^+_{100}, $\sigma^+_{010+001}$, and σ^+ as given by Eq. (1). Calculated cross sections σ^+_{000} and σ^+_{010} are also given by solid and dotted curves, respectively. The measured σ^+_{100} and $\sigma^+_{010+001}$, and calculated σ^+_{010}, have been multiplied by 4 in the figure. The energy scale of the calculated cross sections has been shifted downward 4.0 eV to make the maximum of the calculated σ^+_{000} cross section coincide with the measurement. The kinetic energy scale is the difference between the photon energy and the (0,0,0) threshold energy of 294.352 eV [27]. The vertical scale has been set in such a way that measured and calculated (000) cross sections have the same maximum.

$$\sigma^+ = \sigma^+_{000} + \sigma^+_{010+001} + \sigma^+_{100} + \sigma^+_{110+101} + \sigma^+_{200} + \sigma^+_{210+201}.$$

(1)

The adiabatic cross section σ^+_{000} dominates in the main photoline in Fig. 1. The σ^* shape resonance is seen clearly in the spectral dependence of all partial cross sections in Fig. 2. The cross section σ^+ exhibits the shape resonance at the excess energy of 5.8 eV ($h\nu$=300.2 eV), σ^+_{000} at 6.0 eV ($h\nu$=300.4 eV), σ^+_{100} at 6.0 eV ($h\nu$=300.4 eV), and $\sigma^+_{001+010}$ at 5.4 eV ($h\nu$=299.8 eV). These excess energies, expressed as the difference between the photon energy and the C 1s (0,0,0) threshold of 294.352 eV [12], were extracted by a Gaussian fit of the strongest points in the partial cross sections of Fig. 2, and are precise to 0.1 eV or better. The shape resonance energy in $\sigma^+_{010+001}$ is noticeably lower than those of σ^+_{000} and σ^+_{100}. This v' dependence is similar to the case of the C $1s^{-1}$ σ^* shape resonance in CO [27], where the σ^* shape resonance moves toward the C 1s threshold with an increase of the vibrational C-O stretching excitations.

III. THEORY

The C 1s SHI cross section $\sigma^+_{v'}$ for the individual vibrational component v' is proportional to

$|\int\int \Phi_f^*(r,R)r\Phi_i(r,R)dr\,dR|^2$. In the Born-Oppenheimer approximation the molecular wave functions of the ground (initial) Φ_i and ionic (final) Φ_f states are described as products of the functions $\Psi(r,R)$ and $X_{\mathrm{vib}}(R)$ for the electronic and vibrational motions, where r and R are the electronic and nuclear coordinates, respectively. We assume here that there is no vibrational excitation in the ground state, $v''=0$. The functions $X_{v'}(R)$ and $X_0(R)$ change drastically within the Franck-Condon (FC) region. The R dependence of the electronic wave function is, on the other hand, very smooth and thus the integration over r in the calculation of $\sigma_{v'}^+$ is often performed under the assumption that Ψ is independent of R for the region of the zero-point vibrational distribution in the ground state. The choice of R in defining the FC region should not influence $\sigma_{v'}^+$, because of weak dependence of the electronic function on R. Within this fixed-nuclei (FN) approximation, the C $1s$ SHI cross section $\sigma_{v'}^+$ is a product of the electronic cross section $\sigma^+(E_{v'}|R_e)$ found at the FN geometry and the FC factor $|F_{v'}|^2$, where $F_{v'}=\int X_{v'}^* X_0\,dR$. The FC factor gives the vibrational distribution and thus the v' dependence of $\sigma_{v'}^+$, as long as the vibrational energy is much smaller than the photoelectron kinetic energy, $E_{v'}\gg\Delta_{\mathrm{vib}}=E_{v'}-E_0$.

Dehmer and co-workers [2] have pointed out that the FN approximation does not hold for diatomic molecules in the shape resonance regions because here the photoelectron wave function Ψ_E depends significantly on the internuclear distance. This R dependence of Ψ_E is a natural consequence of the intramolecular interference. The connection between the R-dependent interferential picture and the final vibrational component can be found by examining the matrix elements $\int\int \Phi_f^*(r,R)r\Phi_i(r,R)dr\,dR$, as discussed in detail for CO by Mistrov *et al.* [4]. In particular, for small displacements u of the nuclear separation from the equilibrium distance R^+, one may define a characteristic internuclear distance $R^+(v')$ in the core-ionized molecule for each v' as

$$R^+(v') = R^+ + \frac{1}{F_{v'}}\int X_{v'}^* u X_0\,du. \qquad (2)$$

The second term in the right-hand side of Eq. (2) describes the effective linear displacement responsible for the v' dependence of the molecular geometry. Then the C $1s$ SHI cross section for the individual vibrational component is computed within the geometry fixed at $R^+(v')$. This approximation is called the v'-dependent FN (denoted hereafter as VDFN) approximation. The FN approximation is valid when the effective linear displacement is negligible.

We have computed the characteristic internuclear C-O distances $R^+(v_2')$ using Eq. (2) for C $1s$ ionization in H_2CO for the individual v_2'. The molecular vibrational functions $X_{v_2'}$ and X_0 of the ionic and ground states are approximated to eigenfunctions of the harmonic oscillator in the vicinity of the equilibrium positions R_e and R^+ in the ground and C $1s$ ionized states, respectively. The equilibrium distance for the ground state is 1.2072 Å [36]. The equilibrium distance for the C $1s$ ionized state is obtained to be 1.188 Å in such a way that the ratio of the FC factors $|F_{010}|^2/|F_{000}|^2$ is equal to

the intensity ratio 0.061 of $\{(0,1,0)+(0,0,1)\}$ to $(0,0,0)$ measured at the photon energy of $\simeq 400$ eV. Here we have assumed that the contribution from $(0,0,v_3)$ is negligible, following the analysis of the Rydberg members by Remmers *et al.* [12]. The calculated distances $R^+(v_2')$ using these approximations and assumptions are 1.198, 1.350, and 1.415 Å for $(0,0,0)$, $(0,1,0)$, and $(0,2,0)$, respectively. Thus we have the relation

$$R^+ < R^+(0,0,0) < R^+(0,1,0) < R^+(0,2,0). \qquad (3)$$

The characteristic internuclear C-O distance $R^+(v_2')$ is larger than the equilibrium distance R^+ and increases with an increase in the C-O stretching vibration v_2'.

As a consequence of the vibrational effects on the shape resonance its energy position cannot be unambiguously connected to the equilibrium distance. By inspecting the computed distances $R^+(v_2')$ for $v_2'>0$ we see that they are close to the turning points on the potential curve of the ionic state. For $v_2'=0$ the characteristic interatomic distance can be approximately described as $R^+(0)\simeq(1/2)(R_e+R^+)$. This clearly shows that the energy of the shape resonance for the strongest component ($v_2'=0$) depends on the equilibrium distances in both the neutral ground and core-ionized states.

Within the VDFN approximation, the SHI cross section for individual vibrational component is given by [4]

$$\sigma_{v'}^+ = \sum \sigma_{v',\Gamma}^+(E_{v'}) = \sigma_0|F_{v'}|^2\sum_\Gamma M_\Gamma(E_{v'},R^+(v')), \qquad (4)$$

where $M_\Gamma(E_{v'},R^+(v'))$ describes the interference of the photoelectron wave with kinetic energy $E_{v'}$ within the core-ionized molecule whose C-O distance is equal to $R^+(v')$:

$$M_\Gamma(E_{v'},R_{v'}^+) = \mathrm{Re}\left[\frac{1+B_{v'}S}{1-B_{v'}S}\right]_{11\Gamma}, \qquad (5)$$

where S and $B_{v'}$ are the scattering and reflection matrices, respectively [4]. The interference functions $M_\Gamma(E_{v'},R^+(v'))$ are different for individual vibrational components because of the difference in the characteristic internuclear distances $R^+(v')$. The sum over Γ includes all the dipole-allowed transitions, $\Gamma=a_1$, b_1, and b_2. For C $1s$ photoemission in H_2CO, the multiple-scattering effect is maximum in the $2a_1\to Ea_1$ transition and plays a minor role in $2a_1\to Eb_1$ and $2a_1\to Eb_2$. Thus, we have $M_\Gamma(E_{v'})\simeq M_\Gamma(E_0)\approx 1$ for $\Gamma=b_1$ and b_2.

Using Eqs. (4) and (5), we have computed the C $1s$ SHI partial cross sections of H_2CO for the $(0,0,0)$ and $(0,1,0)$ components in the vicinity of the σ^* shape resonance, under the same approximations as made for CO [4]. The cross sections $\sigma_{v_2'}^+$ thus computed are compared with the measured ones in Fig. 2. The partial cross sections $\sigma_{v'}^+$ are computed also integrating over dR_{CO} [see Eq. (9) in [4]]: the agreement between the two theoretical spectra confirms the validity of the VDFN approximation. Then reasonable agreement between the theoretical and experimental cross sections are obtained. The downward shift of the shape resonance energy by the vibrational excitation $E(0,1,0)-E(0,0,0)\approx-1.0$ eV is close to the measured energy shift of ≈-0.6 eV between the

TABLE I. Changes in the fixed-nuclei geometry and the energy of the shape resonance for individual vibrational components referring to the C-O stretching vibration (v' or v_2'), for the C 1s main line in CO (Ref. [4]) and H_2CO.

Molecule	v' or v_2'	$R^+(v') - R^+$ (Å)	Δ (eV)
CO	$v'=0$	0.025	0.0
	$v'=1$	0.068	-0.8
	$v'=2$	0.111	-1.7
H_2CO	$v_2'=0$	0.009	0.0
	$v_2'=1$	0.162	-1.0
	$v_2'=2$	0.226	-1.3

resonances in σ_{000}^+ and $\sigma_{010+001}^+$. The downward shift of the σ^* shape resonance can be described in terms of the trapping of the C 1s photoelectron by the residual molecular ion elongated in comparison with its equilibrium geometry. The v_2' dependence of the shape resonance energy comes from the intramolecular interference within the vibrating molecular ion. The σ^* shape resonance observed in the C 1s photoemission spectra of H_2CO is regarded as a trap of the C 1s photoelectron by the H_2CO^+ ion whose geometry is fixed at $R^+(v_2')$. The characteristic C-O internuclear distance increases with an increase in the C-O stretching vibrational quantum number v_2'. In contrast to the FN approximation the vibrational dependence of the C 1s SHI cross section of H_2CO is determined not only by the FC factors but also by the difference in the molecular geometry of the trapping ion. The shape resonance position in the total C 1s SHI cross section σ^+ does not coincide with the positions observed for individual vibrational bands.

IV. DISCUSSION

We first focus on the resemblance of the vibrational effect on the C 1s SHI spectral behavior of the H_2CO and CO molecules. For both H_2CO and CO, the shape resonance energy shifts downward with an increase of the quantum number referring to the C-O stretching vibrations. The changes in the characteristic internuclear C-O distances and energy positions of the shape resonance for different vibrational components in the C 1s XPS band in H_2CO and CO are compared in Table I. In numerous x-ray spectroscopic applications, the energy of the σ^* shape resonance is regarded as a measure of the chemical bond length [14,15]. In the SHI spectra of H_2CO and CO, the σ^* shape resonances appear at about 5.8 and 10.4 eV above the C 1s thresholds, respectively. This difference can be attributed to the increase in the C-O bond length in H_2CO compared with CO. The efforts to obtain the bond length from the shape resonance energy have encountered difficulties because the shape resonance energy in the absorption and SHI cross sections turned out to be different, due to many-electron effects, in many molecules [1]. Our results reveal that, in addition to many-electron effects, the energy of the σ^* shape resonance is noticeably influenced by the vibrational excitations accompanying inner-shell ionization.
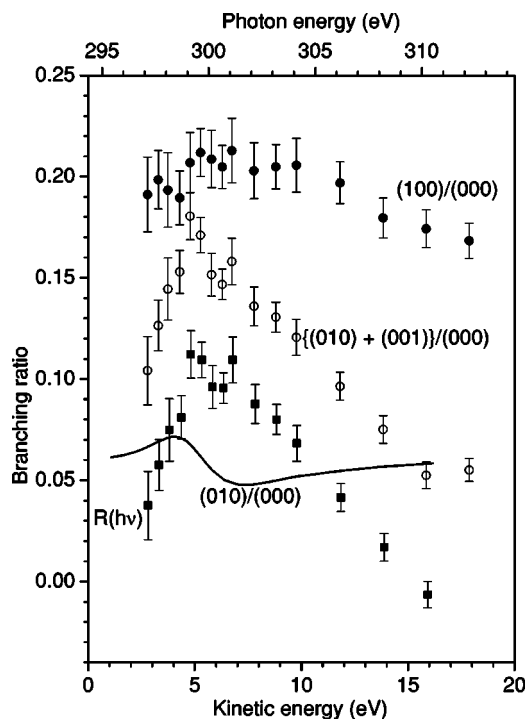

FIG. 3. Vibrational intensity ratios. Full and white circles are measured $[(1,0,0)/(0,0,0)]$ and $[(0,1,0)+(0,0,1)/(0,0,0)]$, the line is the computed branching ratio $[(0,1,0)/(0,0,0)]$, the full squares are the difference between the measured $[\{(0,1,0)+(0,0,1)\}/(0,0,0)]$ and the calculated $[(0,1,0)/(0,0,0)]$ ratios.

In the H_2CO molecule, in addition to the C-O stretching vibrations, the CH_2 scissor and the C-H stretching vibrations may affect the C 1s photoemission dynamics. We now discuss possible general mechanisms, applicable to any mode, that can be responsible for the enhancement of vibrational excitation near threshold and through the shape resonance. In Fig. 3, we present the measured vibrational intensity ratios $[(1,0,0)/(0,0,0)]$ and $[\{(0,1,0)+(0,0,1)\}/(0,0,0)]$, as functions of the incident photon energy. The $[(1,0,0)/(0,0,0)]$ ratio is nearly constant, as for the C-H stretching vibration in C_2H_4 [37]; it increases weakly in the region of the shape resonance as shown in Fig. 3. On the contrary, the ratio $[\{(0,1,0)+(0,0,1)\}/(0,0,0)]$ varies dramatically across the shape resonance, again similarly to the overlapped C-C stretching and CH_2 scissor modes in C_2H_4 [37], though in C_2H_4 the ratio increases monotonically toward threshold.

The variation of these intensity ratios cannot be understood within the FN approximation because within this approximation these ratios are determined by the ratios of the FC factors: $K_{0v'} = |F_{v_2'}|^2/|F_0|^2$. The ratio $[v'/0]$ is energy independent in the region where $E_{v'} \gg \Delta_{vib}$ holds, since here the shape resonance does not influence the distribution of vibrational excitations and $[v'/0] = K_{0v'}$. The vibrational distribution can then be described with the help of the Ansbacher formula [38] and reasonably approximated by a Poissonian distribution.

Within the VDFN approximation, in addition to the $K_{0v'}$ factor, the changes in intramolecular interference for v' com-

ponents affect the intensity ratio. From Eq. (4), it follows that

$$[v'/0] \simeq K_{0v'} \frac{2 + M_{a_1}(E_{v'}, R^+(v'))}{2 + M_{a_1}(E_0, R^+(0))}. \tag{6}$$

Equation (6) describes how the interference effect in the $2a_1 \rightarrow Ea_1$ transition changes the ratios from the ratio of the FC factors, $K_{0v'}$. Far from the ionization threshold, the amplitudes of backscattered photoelectron waves are small and the intramolecular interference plays a minor role in the spectral dependence of inner-shell photoemission; in such a limit the ratio $[v'/0]$ becomes energy independent and the vibrational distribution approaches the Poissonian distribution.

Using Eq. (6) and the computed characteristic internuclear distances, the ratio $[(0,1,0)/(0,0,0)](h\nu)$ is computed. This ratio, presented in Fig. 3, varies in the vicinity of the shape resonance, demonstrating the influence of intramolecular interference on the distributions of the C-O stretching vibrational excitations in the residual ion. The computed spectral variations of the ratio $[(0,1,0)/(0,0,0)](h\nu)$ are, however, rather smooth in comparison with the measured ratio $[\{(0,1,0)+(0,0,1)\}/(0,0,0)](h\nu)$. Thus the measured spectral variation cannot be fully explained within the VDFN approximation in which the elastic multiple scattering is taken into account within the C-O bond-length-dependent scattering potential box.

For further discussion, we made a subtraction of the computed ratio $[(0,1,0)/(0,0,0)](h\nu)$ from the measured ratio $[\{(0,1,0)+(0,0,1)\}/(0,0,0)](h\nu)$:

$$R(h\nu) = [\{(0,1,0)+(0,0,1)\}/(0,0,0)](h\nu)$$
$$- [(0,1,0)/(0,0,0)](h\nu). \tag{7}$$

The subtraction $R(h\nu)$ is also presented in Fig. 3. The enhancement of $R(h\nu)$ is significant in the vicinity of the shape resonance. Examining its spectral behavior in detail, we see that it peaks at the energy of 0.6 eV higher than the energy of the peak of $\sigma^+_{010+001}$. We consider $R(h\nu)$ as representing the contribution beyond the elastic multiple scattering. Below some plausible mechanisms are discussed.

The first is tunneling of the C 1s photoelectron through the potential barrier into the continuum. MacColl [39] pointed out in 1932 that tunneling is not only characterized by a tunneling rate, but also by a time during which the particle is actually traversing the barrier. Since then there have been many investigations of this problem, and we will cite only a few [40,41]. The idea is as follows: a time-dependent barrier $W(r,R,t)$ can be presented as

$$W(r,R,t) = W_0(r,R) + W_1(r,R)\cos(\omega_{\text{vib}}t), \tag{8}$$

where W_0 is a static component and $W_1(r,R)$ is the amplitude of a small modulation of the barrier due to molecular vibrations. Tunneling of the particles with kinetic energy E through the barrier given by Eq. (8) gives rise to "sidebands"

describing the particles with energies $E \pm n\omega_{\text{vib}}$, where $n = 0, 1, 2, \ldots$ [40,42]. This inelastic effect may play an important role in SHI when the traversal time τ is larger than or comparable to the period T of molecular vibrations. For a broad shape resonance, where τ is much shorter than T, or the shape resonance width is much broader than the vibrational spacing, as in the H_2CO and CO cases concerned here, however, the contribution of the "sidebands" to the distribution of vibrational excitations is expected to be rather small.

The second mechanism is connected to internal inelastic scattering. Recent core-level photoemission studies have revealed that the internal inelastic scattering of the photoelectron on valence electrons results in noticeable changes in the SHI cross section at the $4\sigma^*_u$ (Σ_u) shape resonance of CO_2 [43–46] and the e^*_g shape resonance of SF_6 [47,48]. Internal inelastic scattering of the photoelectron on vibrations in the residual ion also influences the distribution of the vibrational excitations. If this is the case, such inelastic scattering may explain the characteristic spectral behavior of $R(h\nu)$.

Doubly excited states autoionizing into the C 1s continuum may fall into the region we investigated and may also provoke deviations from the Poissonian distribution. These states are, however, much more localized than the broad shape resonance and thus the peculiar spectral variation of $R(h\nu)$ in a wide range cannot be attributed to these states.

V. CONCLUSIONS

The vibrationally resolved C 1s SHI cross sections of H_2CO in the region of the σ^* shape resonance are presented. We found that the shape resonance energy moves toward threshold with an increase in C-O stretching vibrational excitations. Our calculations, which take into account the elastic multiple scattering within the C-O potential box, have shown that this downward shift of the shape resonance energy originates from the elongation of the characteristic internuclear C-O distance in the C 1s ionized molecule with an increase in v'_2. The characteristic internuclear distance varies significantly from $R^+(0,0,0) = 1.198$ Å up to $R^+(0,2,0) = 1.415$ Å. The σ^* shape resonance in the SHI cross section for individual vibrational components can be regarded as a trap of the ejected photoelectron by the molecular ion, whose characteristic internuclear distance increases when the vibrational excitation is increased. The enhancement of the intensity ratio of the C-O stretching and/or CH_2 scissor vibrations near threshold and through the shape resonance region cannot be explained within the elastic multiple-scattering model. Internal inelastic scattering of the photoelectron is suggested as a possible explanation.

[1] M. N. Piancastelli, J. Electron Spectrosc. Relat. Phenom. **100**, 167 (1999).

[2] L. Dehmer, D. Dill, and A. C. Parr, in *Photophysics and Photochemistry in the Vacuum Ultraviolet*, edited by S. McGlynn, G. Findly, and R. Huebner (Reidel, Dordrecht, 1985), p. 341.

[3] H. M. Köppe, B. Kempgens, A. L. D. Kilcoyne, J. Feldhaus, and A. M. Bradshaw, Chem. Phys. Lett. **260**, 223 (1996).

[4] D. A. Mistrov, A. De Fanis, M. Kitajima, M. Hoshino, H. Shindo, T. Tanaka, Y. Tamenori, H. Tanaka, A. A. Pavlychev, and K. Ueda, Phys. Rev. A **68**, 022508 (2003).

[5] J. Adachi, K. Hosaka, S. Furuya, K. Soejima, M. Takahashi, A. Yagishita, S. K. Semenov, and N. A. Cherepkov, Phys. Rev. Lett. **91**, 163001 (2003).

[6] S. K. Semenov, N. A. Cherepkov, T. Jahnke, and R. Dörner, J. Phys. B **37**, 1331 (2004).

[7] A. D. Baker, C. Baker, C. R. Brundle, and D. W. Turner, Int. J. Mass Spectrom. Ion Phys. **1**, 285 (1968).

[8] K. Siegbahn, C. Nordling, G. Johansson, J. Hedman, P. F. Heden, K. Hamrin, U. Gelius, T. Berkmark, L. O. Werme, R. Manne, and Y. Baer, in *ESCA Applied to Free Molecules* (North-Holland, Amsterdam, 1969).

[9] U. Gelius, S. Svensson, H. Siegbahn, E. Basilier, Å. Faxälv, and K. Siegbahn, Chem. Phys. Lett. **28**, 1 (1974).

[10] B. Niu, D. A. Shirley, and Y. Bai, J. Chem. Phys. **98**, 437 (1993).

[11] A. P. Hitchcock and C. E. Brion, J. Electron Spectrosc. Relat. Phenom. **19**, 231 (1980).

[12] G. Remmers, M. Domke, A. Puschmann, T. Mandel, C. Xue, G. Kaindl, E. Hudson, and D. A. Shirley, Phys. Rev. A **46**, 3935 (1992).

[13] A. L. D. Kilcoyne, M. Schmidbauer, A. Koch, K. J. Randall, and J. Feldhaus, J. Chem. Phys. **98**, 6735 (1993).

[14] J. Stöhr, *NEXAFS Spectroscopy* (Springer, Berlin, 1992).

[15] F. Sette, J. Stöhr, and A. P. Hitchcock, J. Chem. Phys. **81**, 4906 (1984)

[16] H. Ohashi, E. Ishiguro, Y. Tamenori, H. Kishimoto, M. Tanaka, M. Irie, T. Tanaka, and T. Ishikawa, Nucl. Instrum. Methods Phys. Res. A **467-468**, 529 (2001).

[17] H. Ohashi, E. Ishiguro, Y. Tamenori, H. Okumura, A. Hiraya, H. Yoshida, Y. Senba, K. Okada, N. Saito, I. H. Suzuki, K. Ueda, T. Ibuki, S. Nagaoka, I. Koyano, and T. Ishikawa, Nucl. Instrum. Methods Phys. Res. A **467-468**, 533 (2001).

[18] T. Tanaka and H. Kitamura, J. Synchrotron Radiat. **3**, 47 (1996).

[19] H. Yoshida, Y. Senba, M. Morita, T. Goya, A. De Fanis, N. Saito, K. Ueda, Y. Tamenori, and H. Ohashi, in Proceedings of the Eighth International Conference on Synchrotron Radiation Instrumentation, edited by T. Warwick, J. Arthur, H. A. Padmore, and J. Stöhr, AIP Conf. Proc. **705**, 267 (2004).

[20] Y. Shimizu, H. Yoshida, K. Okada, Y. Muramatsu, N. Saito, H. Ohashi, Y. Tamenori, S. Fritzsche, N. M. Kabachnik, H. Tanaka, and K. Ueda, J. Phys. B **33**, L685 (2000).

[21] T. Shimanouchi, in *Tables of Molecular Vibrational Frequencies Consolidated*, Vol. II, special issue of J. Phys. Chem. Ref. Data **6**, 993 (1972).

[22] P. van der Straten, R. Morgenstern, and A. Niehaus, Z. Phys. D: At., Mol. Clusters **8**, 35 (1988).

[23] H. M. Köppe, A. L. D. Kilcoyne, J. Feldhaus, and A. M. Bradshaw, J. Electron Spectrosc. Relat. Phenom. **75**, 97 (1995).

[24] T. X. Carroll, K. J. Børve, L. J. Sæthre, J. D. Bozek, E. Kukk, J. A. Hahne, and D. T. Thomas, J. Chem. Phys. **116**, 10221 (2002).

[25] A. Kivimäki, B. Kempgens, K. Maier, H. M. Köppe, M. N. Piancastelli, M. Neeb, and A. M. Bradshaw, Phys. Rev. Lett. **79**, 998 (1997).

[26] T. X. Carroll, J. Hahne, T. D. Thomas, L. J. Sæthre, N. Berrah, J. Bozek, and E. Kukk, Phys. Rev. A **61**, 042503 (2000).

[27] H. M. Köppe, B. S. Itchkawitz, A. L. D. Kilcoyne, J. Feldhaus, B. Kempgens, A. Kivimäki, M. Neeb, and A. M. Bradshaw, Phys. Rev. A **53**, 4120 (1996).

[28] T. X. Carroll, N. Berrah, J. Bozek, J. Hahne, E. Kukk, L. J. Sæthre, and T. D. Thomas, Phys. Rev. A **59**, 3386 (1999).

[29] U. Hergenhahn, J. Phys. B **37**, R89 (2004).

[30] J. Bozek, T. X. Carroll, J. Hahne, L. J. Sæthre, J. True, and T. D. Thomas, Phys. Rev. A **57**, 157 (1998).

[31] B. Kempgens, A. Kivimäki, B. S. Itchkawitz, H. M. Köppe, M. Schmidbauer, M. Neeb, K. Maier, J. Feldhaus, and A. M. Bradshaw, J. Electron Spectrosc. Relat. Phenom. **75**, 97 (1995).

[32] K. J. Børve, L. J. Sæthre, T. D. Thomas, T. X. Carroll, N. Berrah, J. D. Bozek, and E. Kukk, Phys. Rev. A **63**, 012506 (2000).

[33] E. E. Rennie, H. M. Köppe, B. Kempgens, U. Hergenhahn, A. Kivimäki, K. Maier, M. Neeb, A. Rüdel, and A. M. Bradshaw, J. Phys. B **32**, 2691 (1999).

[34] T. Karlsen, L. J. Sæthre, K. J. Børve, N. Berrah, E. Kukk, J. D. Bozek, T. X. Carroll, and T. D. Thomas, J. Phys. Chem. A **105**, 7700 (2001).

[35] T. D. Thomas, L. J. Sæthre, K. J. Børve, J. D. Bozek, M. Huttula, and E. Kukk, J. Phys. Chem. A **108**, 4983 (2004).

[36] D. J. Clautier and D. A. Ramsey, Annu. Rev. Phys. Chem. **34**, 31 (1983).

[37] S. L. Sorensen, M. Wiklund, S. Sundin, A. Ausmees, A. Kikas, and S. Svensson, Phys. Rev. A **58**, 1879 (1998).

[38] F. Ansbacher, Z. Naturforsch. A **14**, 889 (1959).

[39] L. A. MacColl, Phys. Rev. **40**, 621 (1932).

[40] M. Buttiker, Phys. Rev. B **27**, 6178 (1983).

[41] S. Collins, D. Lowe, J. R. Barker, J. Phys. C **20**, 6213 (1987).

[42] P. K. Tien and J. P. Gordon, Phys. Rev. **129**, 647 (1963).

[43] A. De Fanis, N. Saito, A. A. Pavlychev, D. Yu. Ladonin, M. Machida, K. Kubozuka, I. Koyano, K. Okada, K. Ikejiri, A. Cassimi, A. Czasch, R. Dörner, H. Chiba, Y. Sato, and K. Ueda, Phys. Rev. Lett. **89**, 023006 (2002).

[44] M. Hoshino, T. Tanaka, M. Kitajima, H. Tanaka, A. De Fanis, A. A. Pavlychev, and K. Ueda, J. Phys. B **36**, L381 (2003).

[45] A. De Fanis, N. Saito, K. Okada, M. Machida, I. Koyano, K. Ikejiri, A. Cassimi, A. Czasch, R. Dörner, A. A. Pavlychev, and K. Ueda, J. Electron Spectrosc. Relat. Phenom. **137-140**, 265 (2004).

[46] M. Hoshino, T. Tanaka, M. Kitajima, A. De Fanis, H. Tanaka, A. A. Pavlychev, and K. Ueda, in *Proceedings of VUV14*, edited by Anatoli Kheifets, Maarten Vos, Steven J. Cavanagh, and Mitsu Kono, J. Electron Spectrosc. Relat. Phenom. **144**, 203 (2005).

[47] T. A. Ferrett, D. W. Lindle, P. A. Heimann, H. G. Kerkhoff, U. E. Becker, and D. A. Shirley, Phys. Rev. A **34**, 1916 (1986).

[48] K. Fujiwara, G. Prümper, A. De Fanis, Y. Tamenori, T. Tanaka, H. Shindo, M. Kitajima, H. Tanaka, N. Saito, M. Oura, A. A. Pavlychev, and K. Ueda, in *Proceedings of VUV14* (Ref. [46]).